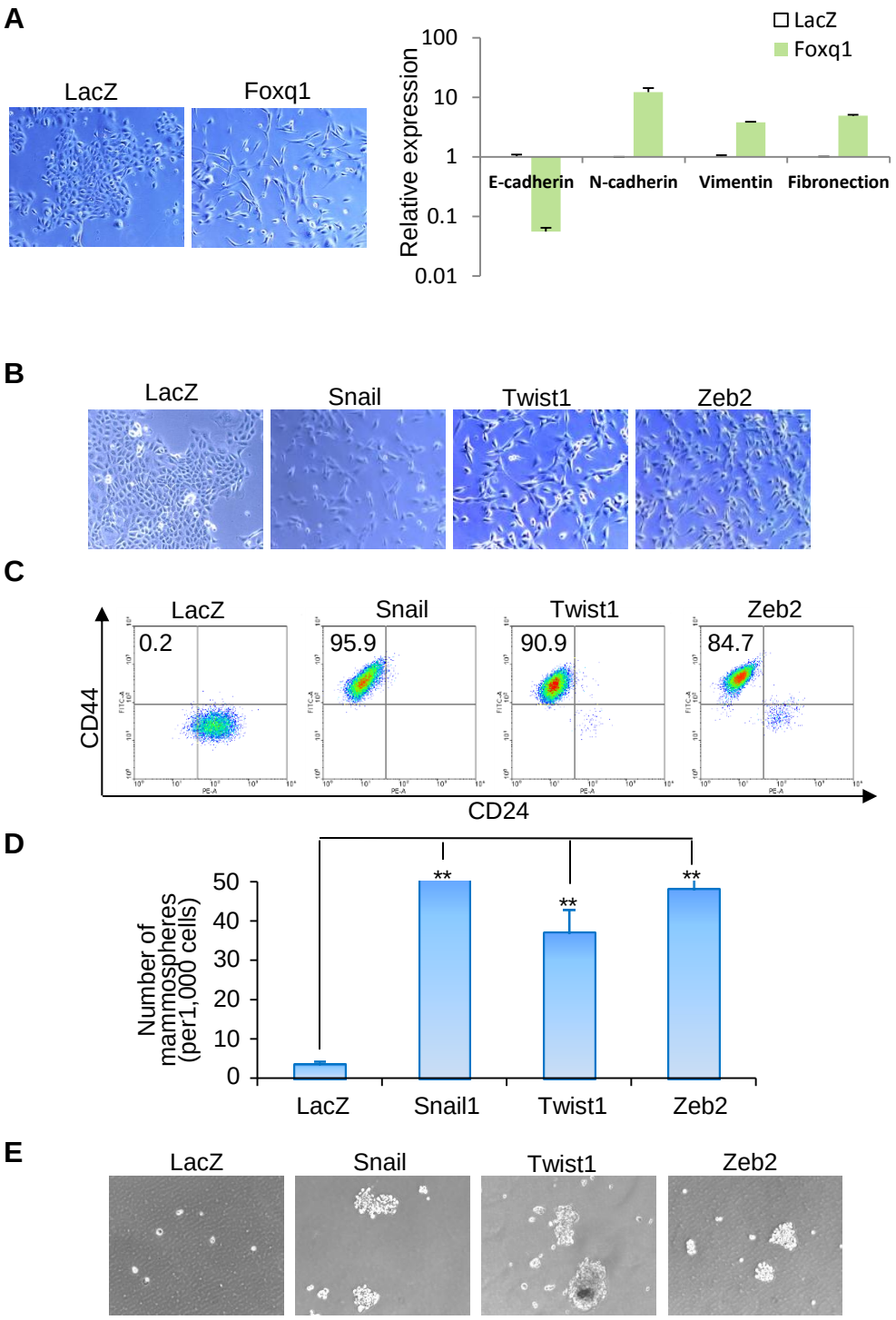

Supplementary Figure S1. EMT promoting transcription factors induce stemness characteristics. **A**, Overexpression of Foxq1 significantly induced EMT in HMLE cells. Left Panel: Morphological change. Right panel: expression of EMT markers. **B**, Overexpression of Snail, Twist1 and Zeb2 significantly induced EMT in HMLE cells. **C**, Overexpression of Snail, Twist1 and Zeb2 significantly increased the $CD44^{high}/CD24^{low}$ cell population in HMLE cells. **D**, Summary of the mammosphere formation assay for Snail1, Twist1 and Zeb2 overexpressing HMLE cells (**P<0.01). **E**, Representative figures for the mammosphere formation assay of Snail1, Twist1 and Zeb2 overexpressed HMLE cells. HMLE cells transfected with LacZ was used as a control.

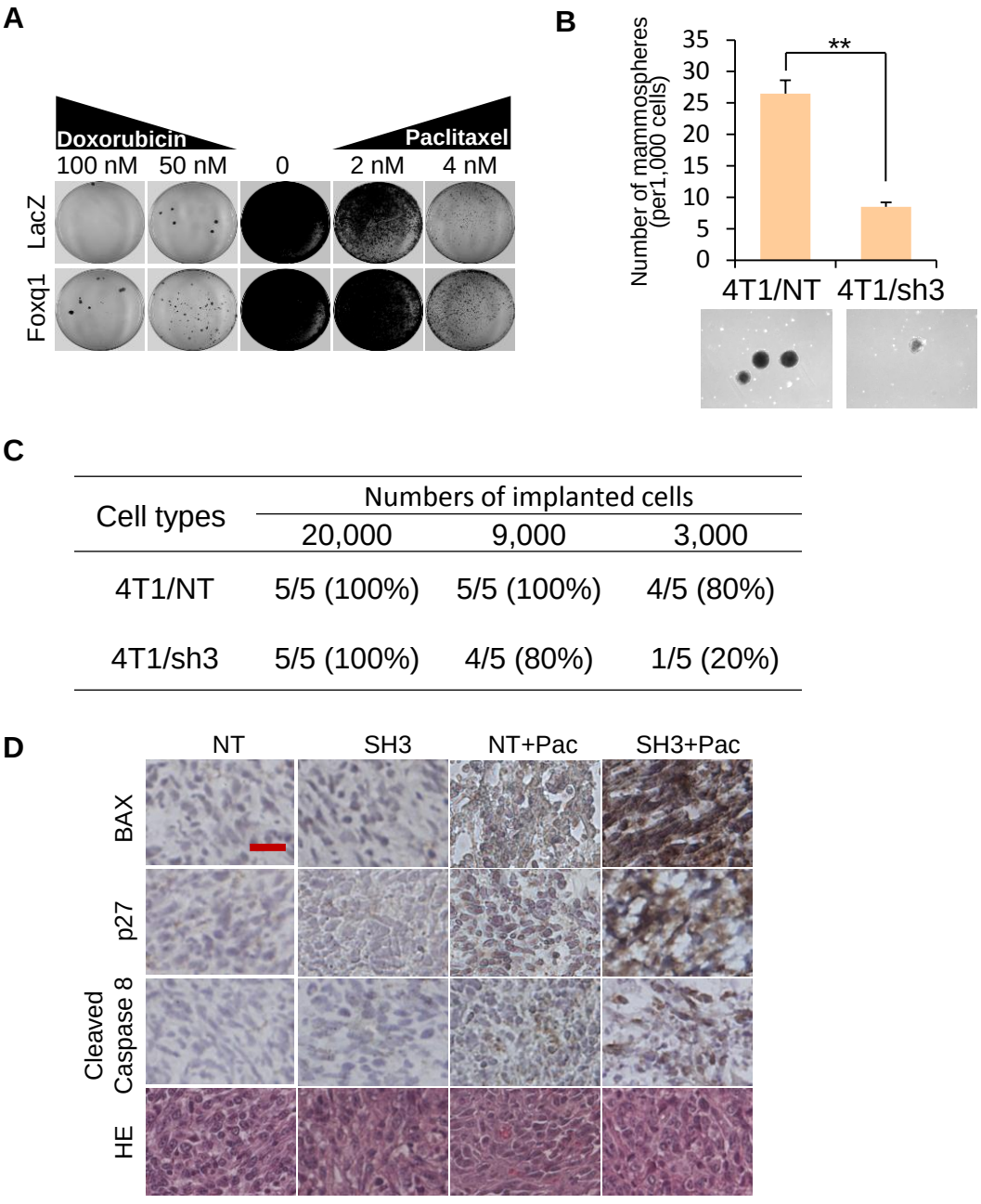

Cell types	Numbers of implanted cells		
	20,000	9,000	3,000
4T1/NT	5/5 (100%)	5/5 (100%)	4/5 (80%)
4T1/sh3	5/5 (100%)	4/5 (80%)	1/5 (20%)

Supplementary Figure S2. The role of Foxq1 in drug resistance, mammosphere formation and tumor initiation. A, Representative images of the clonogenic assays of HMLE cells with or without Foxq1 overexpression treated with different doses of doxorubicin (dox) or paclitaxel (pac). **B**, Knockdown of Foxq1 significantly decrease mammosphere formation ability of 4T1 cells. Top panel: summary of mammosphere formation results. Bottom panels: representative image of mammosphere formation. **C**, Summary of tumor initiation capability of Foxq1 in 4T1 cells. Five mice were used for each group. Percentiles represent tumor formation in specific groups. **D**, The effect of Foxq1 in apoptosis. Tumors were collected from the 4T1 implanted BALB/C mice, and the prepared tissue slides were analyzed with IHC using anti-BAX, p27 and Cleaved Caspase 8 antibodies, as well as H&E staining. The origins of all four tumor samples are indicated at the top of the panels. NT: tumor from 4T1/NT cells bearing mouse. SH3: tumor from 4T1/SH3 Foxq1 knockdown cell bearing mouse. NT+Pac: tumor from 4T1/NT cells bearing mice treated with Paclitaxel. SH3+Pac: tumor from 4T1/Sh3 cells bearing mice treated with Paclitaxel. Scale bar, 20 μm.

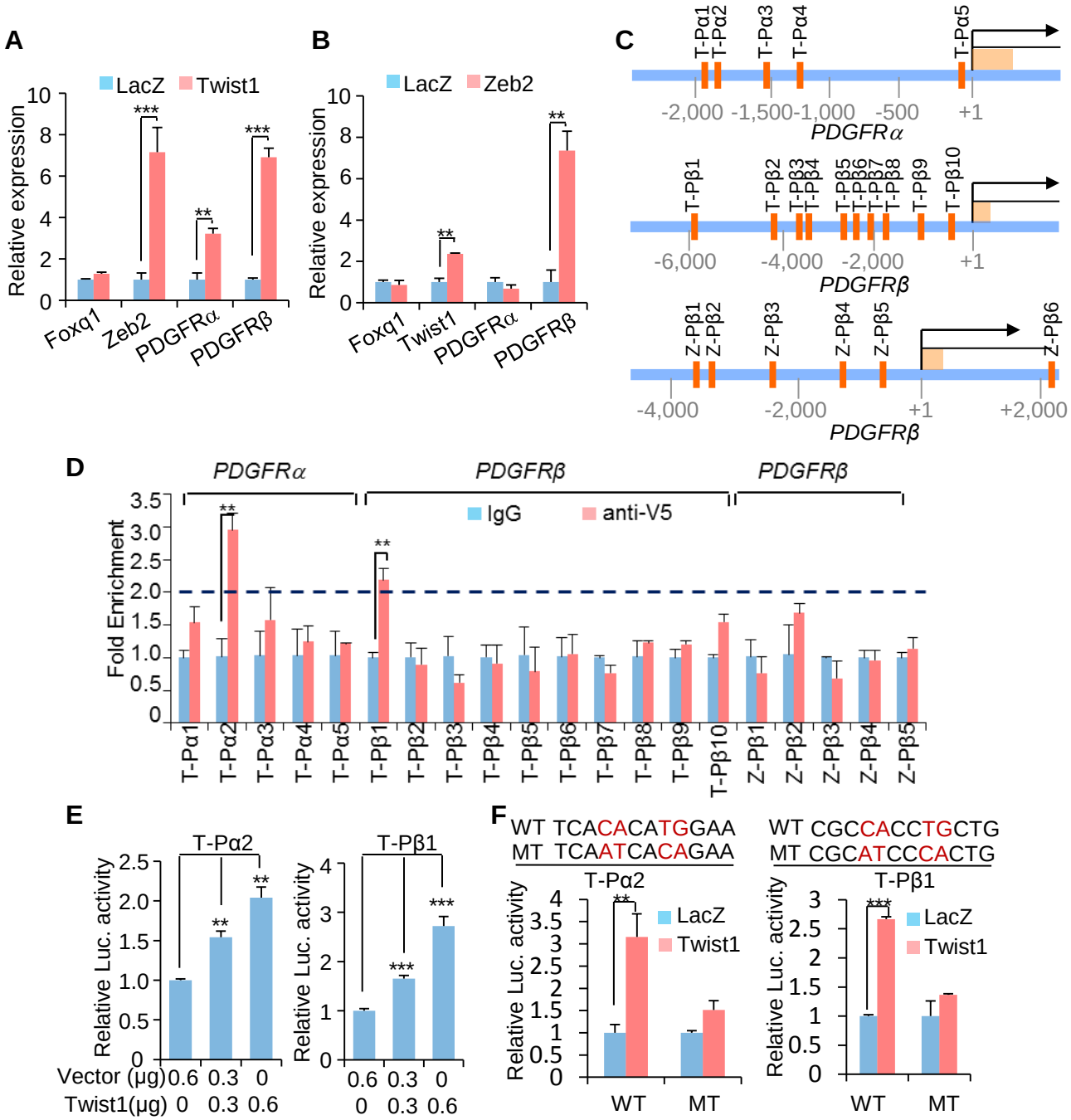

Supplementary Figure S3. Twist1 and Zeb2 regulate PDGFRs. A and B, The relative expression level of the Foxq1, Zeb2/Twist1 and PDGFRα and β genes in Twist1 (A) or Zeb2 (B) overexpressing HMLE cells was measured by real-time RT-PCR assay (*P<0.05, **P<0.01 and ***P<0.001). **C**, Potential binding sites of Twist1 and Zeb2 in the promoter regions of PDGFRα and β genes were identified by an in silico analysis. Top and middle panels show Twist1 binding sites in PDGFRα and β promoter region. Low panel shows Zeb2 binding site in PDGFRβ promoter region. The conserved binding sites are highlighted with red. **D,** ChIP-qPCR analysis shows that enrichment of one Twist1 binding site DNA from the PDGFRα and β promoter region, respectively (**P<0.01). Dotted line represents 2-fold enrichment. However, ChIP-qPCR assay did not show enrichment of DNA for Zeb2 binding in PDGFRβ promoter. **E**, Luciferase assay shows Twist1 activated the PDGFRα (left panel) and β (right panel) gene promoter in a dose-dependent manner (**P<0.01, ***P<0.001). **F**, The binding of Twist1 to the PDGFRα and β promoter region was confirmed by luciferase assay. The Twist1 conservative binding sequence (WT) and mutant sequence (MT) for PDGFRα and β promoters was shown on the top of the panels. The mutation of the binding sequence diminished the activation of both gene promoters by Twist1 (**P<0.01, ***P<0.001).

A

Breast cancer of TCGA database

Pvalue/correlation	FOXQ1	Twist1	PDGFR-A	PDGFR-B
FOXQ1		0.29	0.21	0.16
Twist	4E-14		0.45	0.47
PDGFR-A	4.6E-11	<2.2E-16		0.67
PDGFR-B	3.2E-4	<2.2E-16	<2.2E-16	

B

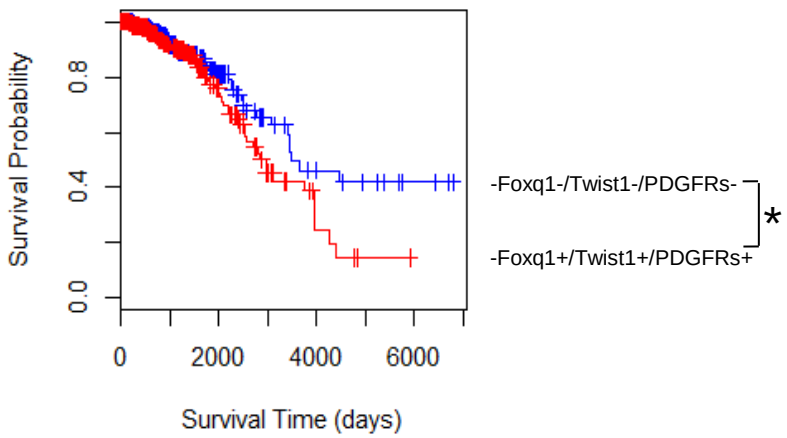

C

UCEC of TCGA database

Pvalue/Correlation	FOXQ1	TWIST1	PDGFRA	PDGFRB
FOXQ1		0.164	0.16	0.143
TWIST1	0.00227		0.375	0.32
PDGFRA	0.0431	2.33E-11		0.709
PDGFRB	0.0107	3.36E-10	0	

Supplementary Figure S4. Correlation and survival analysis of Foxq1 and Twist1 with PDGFRα and PDGFRβ in tumor samples. **A,** The expression correlation of Foxq1 or Twist1 with PDGFRα and β in breast cancer. Level 3 gene expression (RNAseV2) data of breast tumors from The Cancer Genome Atlas (TCGA) database was used for the analysis. In the table, the upper panels (highlighted in green) show correlation coefficients and the lower panels (highlighted in orange) include the corresponding correlation p-values. **B**, The Kaplan-meier plot shows that overexpression of Foxq1 and Twist1 with PDGFRs predicts poor survival of breast cancer patients in TCGA dataset (*P<0.05). **C**, The expression correlation of Foxq1 or Twist1 with PDGFRα and β in Uterine corpus endometrial carcinoma (UCEC). Level 3 gene expression (RNAseV2) data in UCEC from The Cancer Genome Atlas (TCGA) database was used for the analysis. The table setting is same as in panel A.

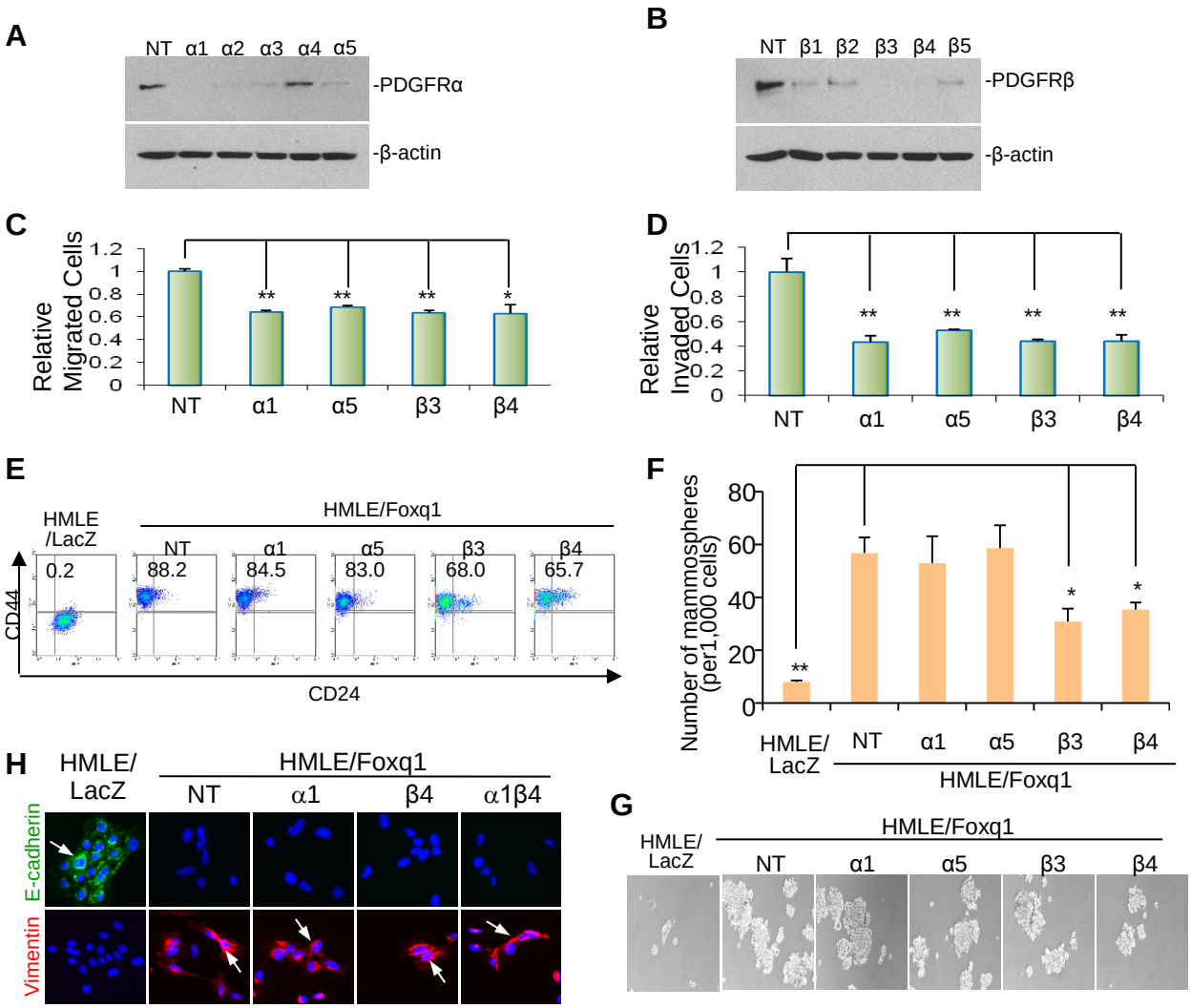

Supplementary Figure S5. Effect of PDGFRα and PDGFRβ on cell migration, invasion and stem cell characteristics. A-B, Knockdown of PDGFRα (A) and PDGFRβ (B) expression in HMLE /Foxq1 cells. Five different shRNAs specifically targeting PDGFRα or β were tested. β-actin was used as a protein loading control. **C-D,** The effect of PDGFRs silencing on cell migration and invasion of HMLE/Foxq1 cells. All stable cell lines with significant inhibition of PDGFRα and β expression showed significant decrease in cell migration (C) (*P<0.05) and invasion (D) (***P*<0.01). **E** Effect of PDGFRs on Foxq1 induced $CD44^{high}/CD24^{low}$ cell population. Two PDGFRα knockdown cells showed minor cell population changes, while two PDGFRβ knockdown cell models showed marked decrease of $CD44^{high}/CD24^{low}$ cell population. **F**, Summary of the effect of PDGFRα and PDGFRβ knockdown on mammosphere formation of HMLE/Foxq1 cells (*P<0.05, **P<0.01). **G**, Representative figures of mammosphere formation of HMLE/Foxq1 cells with PDGFRα and PDGFRβ knockdown. **H**, Immunofluoresence assay showed no expression change of E-cadherin and Vimentin in HMLE/Foxq1 cells with individual and double knockdown of PDGFRα and β.

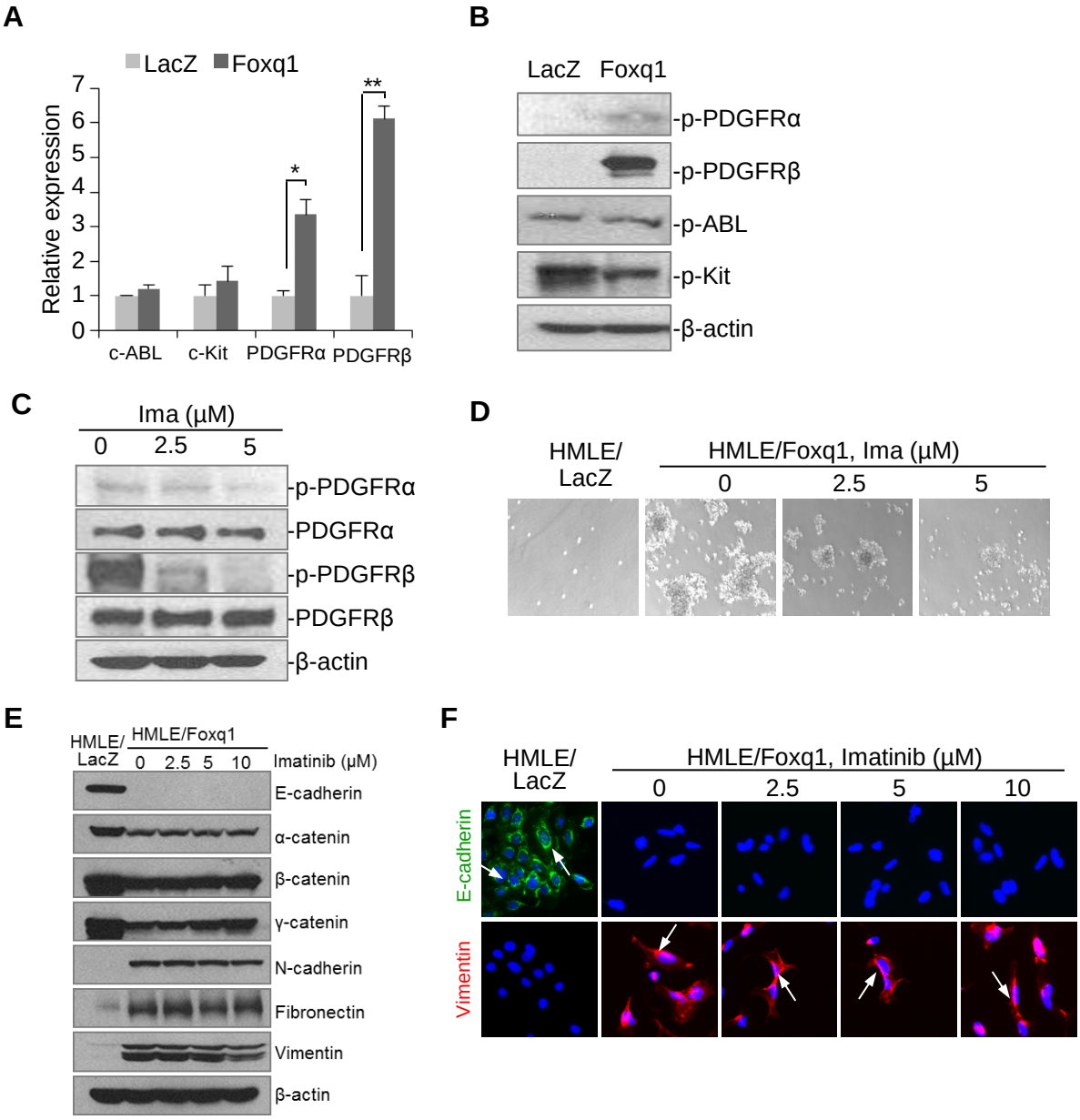

Supplementary Figure S6. Imatinib treatment on PDGFRs phosphorylation, mammosphere formation and EMT. A, The expression of c-abl, kit and PDGFRs in HMLE cells with Foxq1 or control LacZ overexpression was detected by real time RT-PCR (**P*<0.05, ***P*<0.01). **B,** Overexpression of Foxq1 leads to phosphorylation of PDGFRα and β, but not the c-ABL and c-kit. **C,** imatinib (Ima) treatment inhibit phosphorylation of PDGFRs. Western blot analysis was performed using total and phosphor-PDGFRα and β antibodies. **D**, Representative figures for mammosphere formation in HMLE/Foxq1 cells after treatment of different doses of imatinib. **E**, No expression changes for epithelial and mesenchymal markers in HMLE/Foxq1 cells with different doses of imatinib treatment were detected by western blotting assay. **F,** Immunofluoresence assay shows no expression change of E-cadherin and Vimentin proteins in HMLE/Foxq1 cells with different doses of imatinib treatment.

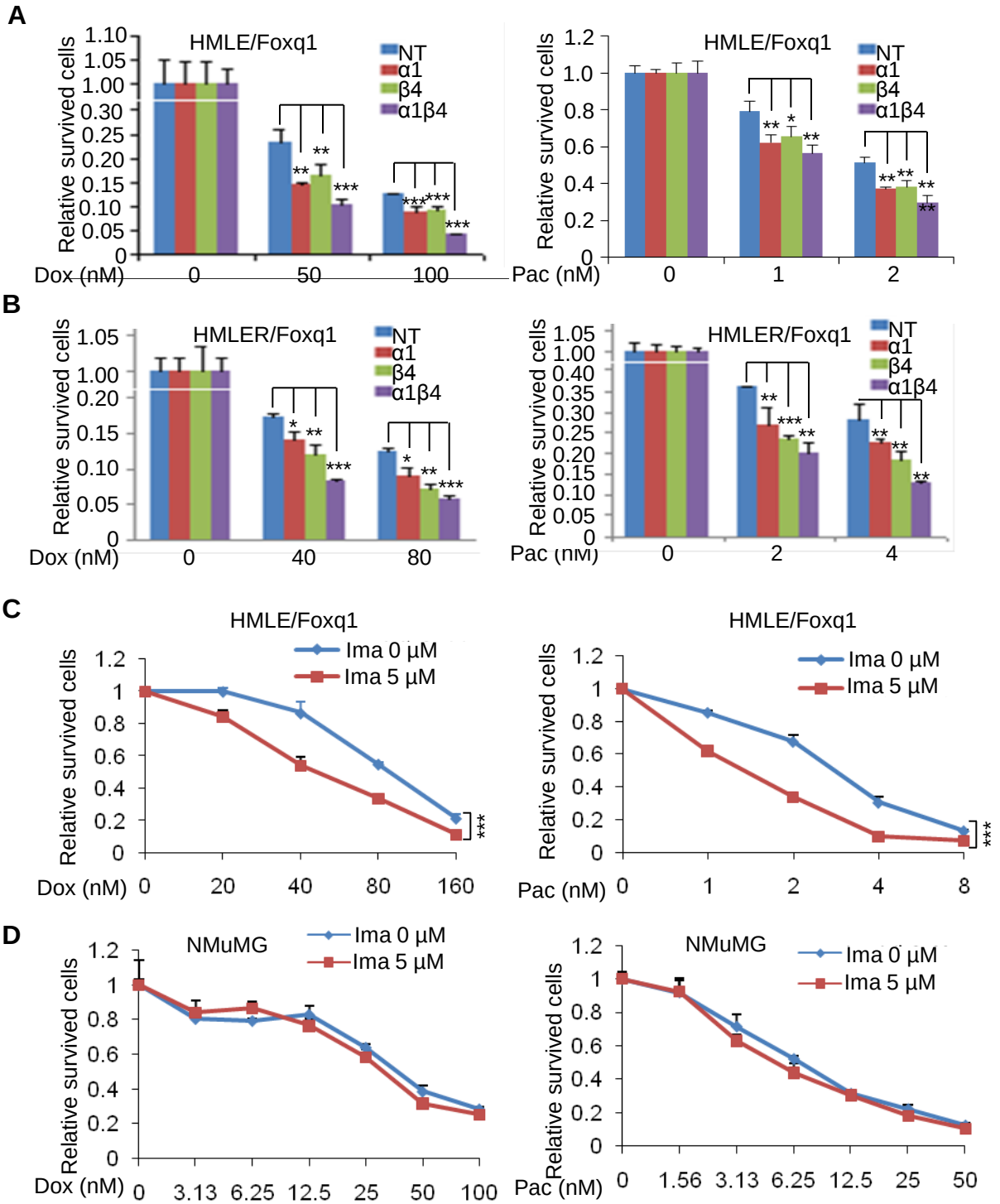

Supplementary Figure S7. The Effect of PDGFRs on chemoresistance. **A and B**, Chemoresistance of HMLE/Foxq1 (A) and HMLER/Foxq1 (B) cells with individual or double PDGFRα and β knockdown was analyzed by an MTT assay after treatment with various doses of doxorubicin left panel) and paclitaxel (right panel). Results are presented as relative cell survival compared to the non-treatment control (**P*<0.05, ***P*<0.01 and ****P*<0.001). **C**, Increased sensitivity of HMLE/Foxq1 cells to doxorubicin (left panel) or paclitaxel (right panel) in the presence of imatinib (****P*<0.001). **D**, NMuMG cells shows no increased sensitivity to doxorubicin (left panel) and paclitaxel (right panel) in the presence of imatinib (*P*>0.05).

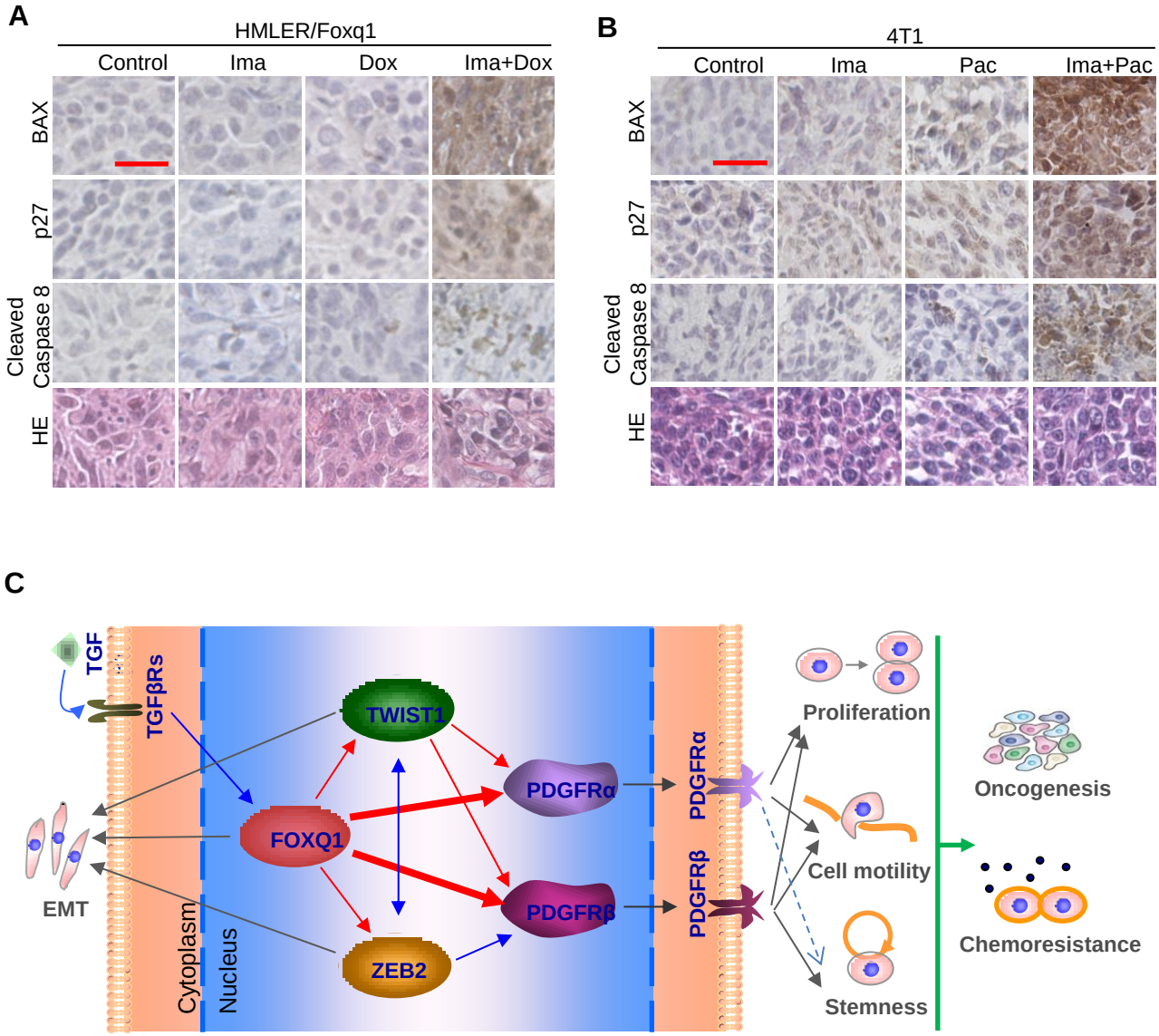

Supplementary Figure S8. Immunohistochemistry (IHC) assays using tumor samples and our working model. A, Tumors were collected from the HMLER/Foxq1 implanted NCR nu/nu mice, and the prepared tissue slides were analyzed with IHC using anti-BAX, p27 and Cleaved Caspase 8 antibodies, as well as H&E staining. The origins of all four tumor samples are indicated at the top of the panels. Scale bar, 50 μm. **B,** Tumors were collected from 4T1 implanted BALB/c mice. The other settings are the same as panel A. **C**. Schematic model of the molecular mechanism underlying Foxq1/PDGFR-driven breast cancer oncogenesis and chemoresistance. Foxq1, an EMT promoting transcription factor, simultaneously regulates PDGFRα and β genes through direct or indirect mechanisms. Twist1 and Zeb2 are the mediators of Foxq1's indirect regulatory mechanism. This study reveals the central regulatory role of Foxq1 in the TGFβ and PDGF signaling transition. Moreover, the results of this study highlight PDGFR as important mediator of Foxq1/Twist1 promoted oncogenesis and chemoresistance, which suggests an implication of designing novel combinational therapy for breast cancer treatment (the dashed line indicates a relationship need further validation of *in vivo* study).